Journal of Medical Devices Technology
jmeditec.utm.my

Original Research

# Permeability of Bone Scaffold with Different Pore Geometries Based on CFD Simulation

Norhana Jusoh[1,2,3*], Muhammad Aqil Mustafa Kamal Arifin[1], Muhammad Hamizan Hilmi Sulaiman[1], Muhammad Aiman Mohd Zaki [1], Nurul Ammira Mohd Noh[1], Nur Afiqah Ahmad Nahran[1], Koshelya Selvaganeson[1], Amy Nurain Syamimi Ali Akbar[1]

[1] *School of Biomedical Engineering and Health Sciences, Faculty of Engineering, Universiti Teknologi Malaysia, 81310 UTM Johor Bahru, Johor, Malaysia*
[2] *Medical Device Technology Center (MEDiTEC), Institute Human Centred Engineering (iHumen), Universiti Teknologi Malaysia, 81310 UTM Johor Bahru, Johor, Malaysia*
[3] *Bioinspired Device and Tissue Engineering Research Group, School of Biomedical Engineering and Health Sciences, Universiti Teknologi Malaysia, 81310 UTM Johor Bahru, Johor, Malaysia*

ARTICLE INFO

*Article History:*
Received 6 September 2022
Accepted 14 September 2022
Available online 30 September 2022

*Keywords:*
Permeability,
Pore Geometry,
Unit cell,
Fluid Simulation,
Bone Scaffold.

ABSTRACT

Scaffold plays a significant role in promoting cells proliferation and differentiation in bone regeneration.Permeability is one of the factors that affect the function as it is able to extract waste and supplynutrients or oxygen. The aim of this study was to design different pore shapes and to simulate its fluid model in order to predict permeability value of the scaffold. There were few steps in this project which were scaffold design, fluid simulation analysis and permeability calculation. Three different pore shapes were designed, which were circle, triangle, and hexagon by using the Solidworks software. Each scaffold was designed by the combination of three unit cells. Then, Computational Fluid Dynamics (CFD) simulation in the Ansys Fluent software was conducted to obtain the pressure drop from the pressure distribution within the pores. The permeability of scaffold was obtained by applying Darcy's permeability formula at inlet velocity of 0.001 m/s, 0.01 m/s and 0.1 m/s. Based on the calculation, the permeability for hexagon pore shape were $3.96691 \times 10^{-07}$ $m^2$, $3.52 \times 10^{-07}$ and $1.92 \times 10^{-07}$ for 0.001 m/s, 0.01 m/s and 0.1 m/s inlet velocity, respectively. Therefore, by increasing the inlet velocities, permeability decreased for all types of scaffolds. Furthermore. hexagon pore shape showed the highest permeability value when compared with triangle and circle's pore shape. Nevertheless, all pore shapes demonstrated permeability values that within the range of natural bone permeability.

## INTRODUCTION

The scaffolds are designed with specific characteristics in order to comply with the physiological nature of the human body especially in tissue and organ regenerations (Li et al., 2014). Scaffold structure must copy the three-dimensional (3D) network of native ECM in tissue in order to provide permanent or temporary support to cells growth (Pei et al., 2017). One important aspect of tissue engineering includes the utilizing of high-porosity scaffolds that serve as temporary three-dimensional models for cell adhesion, proliferation, migration and, eventually, the development of new tissues (Hutmacher et al., 2007). Therefore, the porous bone scaffold is manufactured in such a way as to mimic human natural bone features in terms of structure, mechanical properties, fluid transfer and load bearing. As a result, scaffolds will provide an effective medium for nutrient transfer, tissue ingrowth and differentiation (Hutmacher et al., 2007). As an artificial extracellular matrix (ECM), scaffold plays a significant role in promoting cell proliferation and differentiation (Li et al., 2014).

The design of the scaffold is a complex process by controlling multiple parameters such as mechanical properties (Truscello et al., 2012; Dias et al., 2012), biodegradation (Podichetty and Madihally, 2014), biocompatibility, pore architecture, porosity,

* Norhana Jusoh
Medical Device Technology Center (MEDiTEC), Institute Human Centred Engineering (iHumen), Universiti Teknologi Malaysia, 81310 UTM Johor Bahru, Johor, Malaysia

surface properties and permeability. Permeability is correlated with the amounts of pores that defines the capacity of fluid movement within a porous material with the micro-structural design that related with the ability to extract waste and supply nutrients or oxygen (Ochoa et al., 2009). Therefore, permeability is related with the scaffold's ability to improve the regeneration of tissue. However, higher permeability will influence the high flow rate that eventually reduces the bone development (Singh et al., 2018). However, low permeability will result in cell nutrient supply reduction (Gomez et al., 2016), which delays the growth of the bone. Therefore, the target permeability range is close to a natural bone ($0.5 < k\ (10^{-8}\ m^2) < 5$) (Singh et al., 2018).

Among the various structural properties of these scaffolds, permeability has been shown to be a key parameter that influences tissue regeneration and survival (Vikingsson et al., 2015). Permeability is essentially characterized as the capacity of the porous medium to conduct the flow of fluids, to affect the cell growth and hence the biological efficiency of the porous scaffolds (Daish et al., 2017). Improper scaffold design will affect permeability, causing necrosis areas in the middle of the scaffold and inadequate load bearing properties. Therefore, permeability can be improved by manipulating the pore size, pore shape, porosity, interconnectivity, pore direction and tortuosity. Ochoa et al. (2009) investigated the average permeability using Darcy's law for highly porous bioglass-derived scaffolds fabricated and these scaffolds showed similar values of permeability to those observed in human trabecular bone. In another study, Furumoto et al. (2015) investigated the relationship between the processing state, porosity, tensile strength and gas permeability of porous metal structures formed by selective laser sintering that demonstrated an increase in permeability with porosity (Furumoto et al., 2015).

The challenge in choosing a scaffold design parameter such pore size and shape and porosity others due to the effect of pore architecture on mass transport and ultimately on bone growth (Dias et al., 2012). For example, pore size can affect the pressure within the scaffold and the inlet velocity. Larger pore size will reduce the pressure drop but with the increase of the velocity inlet (Singh et al., 2018). Pressure drop will be higher with the increased of the inlet velocity inlet and increased in pore size (Singh et al., 2018). Furthermore, the pore shape of the bone scaffolds is one of the variables that may influence the permeability.

Computational models of biomaterials have recently attracted considerable exposure to the potential to produce instant outcomes as an alternative and cost-effective solution relative to laboratory analyses (Gomez et al., 2016). Numerous computational fluid dynamics (CFD) analyzes have been performed to determine the permeability of different forms of scaffolds (Melchels et al., 2011). CFD simulations were used to demonstrate that cellular growth in 3D scaffolding that induced an increased in wall shear stress due to contraction in scaffolding channels during perfusion cell culture (Lesman et al., 2016). CFD simulation was employed to study the parametric impacts of the geometric features of scaffolds, such as architecture, pore size, and porosity in the pores employing a fluid–structure interaction model for various cases of loading during fluid perfusion, mechanical compression, as well as a combination of the two (Zhao et al., 2016).

Permeability per unit cell was accepted since permeability is an intrinsic property of a material due to uniform pore distribution. Therefore, in this study, each scaffold was designed by the combination of three unit cells. We designed bone scaffold with different pore shapes which were circle, hexagon and triangle by using Solidworks and we predicted the permeability by CFD simulation in Ansys Software.

## MATERIALS AND METHOD

### Scaffold model design

Solidworks software was used to design the scaffold unit cells. In this step, three different scaffolds were designed based on the pore shape, which were circle, triangle, and hexagon. In this study, each scaffold was designed by the combination of three unit cells for each scaffold, as shown in Figure 1. Scaffold models were designed by SOLIDWORKS software with d defined volume of interest (VOI) of 8.4x2.8x2.8mm for all models. The pore dimensions were 2 mm for all different pore shapes.

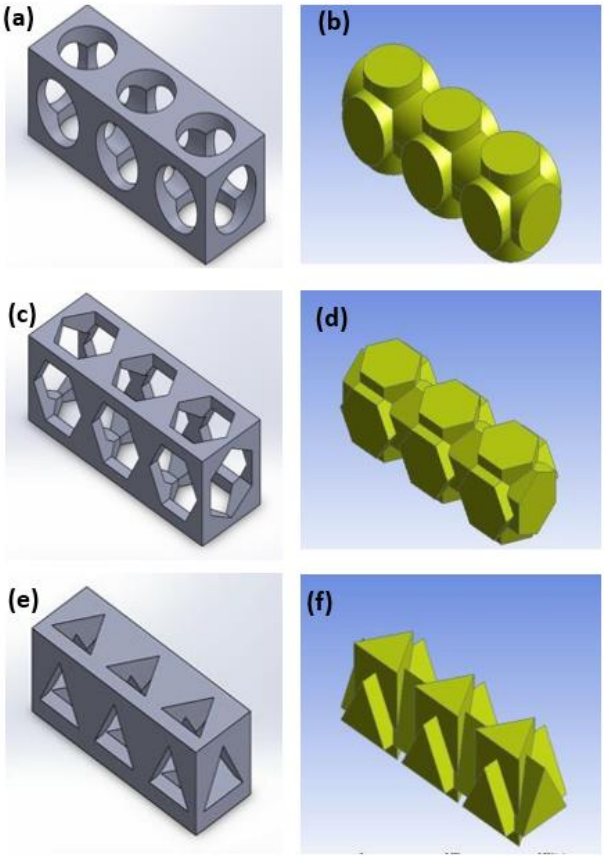


**Fig. 1** Scaffold design (a,c,e) and fluid flow model (b,d,f) for circle (a,b), hexagon (c,d) and triangle (e,f) pore shape

### Fluid simulation

Then, the scaffold solid design was converted to the fluid model by by subtracting the scaffold model from the defined volume of interest (VOI) (Singh et al., 2018). The permeability of all scaffolds was obtained through Computational Fluid Dynamics (CFD) simulation in the Ansys software based on fluid flow (fluent) application. Before the analysis, fluid properties such as the density and viscosity of the fluid were inserted, and boundary conditions such as inlet velocity, outlet pressure, and fluid wall conditions were determined. The meshing was conducted once these conditions and properties were defined.

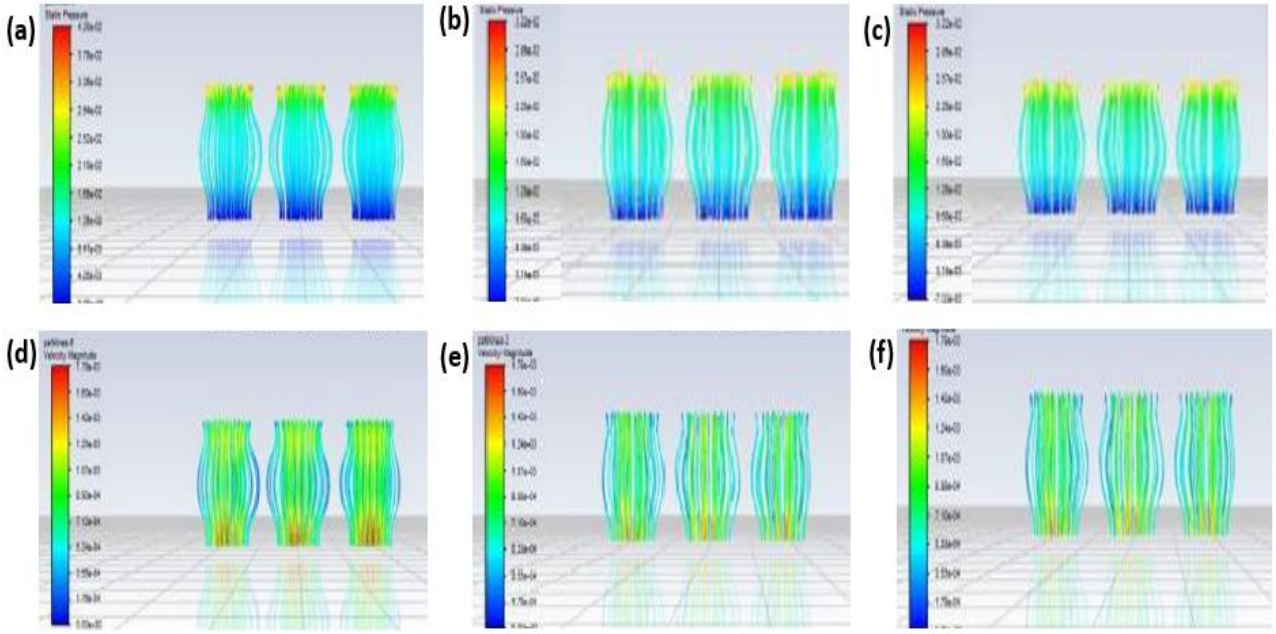


**Fig. 2** Pressure distribution (a-c) and velocity distribution (d-f) for circle (a,d), hexagon (b,e) and triangle (c,f) pore shape at inlet velocity of 0.001m/s.

Dulbecco modified Eagle's minimal essential medium (DMEM) was used as the working fluid with density at 1000 kg/m$^3$ density and viscosity at 0.0015225 Pa.s. Different inlet velocities was applied at the top which were 0.001 m/s, 0.01 m/s and 0.1 m/s. The outlet pressure at the bottom was considered nil and the other surfaces were considered fluid wall conditionwith no slip surface. Then, the simulation was performed at different inlet velocities and the pressure drop across the scaffold was measured.

### Permeability calculation

After the pressure drop for all the scaffold designs was obtained in the simulation, the permeability was calculated by using Darcy's formula as shown in the equation below:

$$K = \vartheta_D . \mu_D . \left(\frac{L}{\Delta P_{i-O}}\right) \qquad (1)$$

where, K= Permeability of unit cell, L= length of fluid model, ΔPi-o= Pressure difference between inlet and outlet $\vartheta_D$= Velocity at inlet and $\mu_D$ = Viscosity of the DMEM Fluid.

## RESULT AND DISCUSSION

By using Solidworks software, scaffold models with different pore shapes which were circle, hexagon and triangle with fixed diameter size at 2mm were successfully designed. Figure 1 shows the scaffold design (a,c,e) and fluid flow model (b,d,f) for circle (a,b), hexagon (c,d) and triangle (e,f) pore shape.

By using ANSYS software, velocity distribution and pressure distribution were determined at different inlet velocities which were 0.001m/s, 0.01m/s and 0.1m/s. Figure 2 shows the pressure distribution and velocity distribution for all types of scaffolds at 0.001m/s as the representative image. From the contour plot of velocity streamline, the maximum velocity magnitudes were observed at different velocities. Circle pore shape showed highest velocity distribution at all different inlet velocities compared to hexagon and triangle that had almost the same velocity reading due structure of the scaffold. Meanwhile, circle pore shape has the smoothest edges of shape compared to other shape. The pressure streamline shows the different pressure at the inlet and outlet region, which create the pressure drop.

**Table 1** Pressure drop for each pore shape at different velocities.

| | Pressure Drop (Pa) | | |
|---|---|---|---|
| **Velocity (m/s)** | **Circle** | **Hexagon** | **Triangle** |
| 0.001 | 0.04204 | 0.032239176 | 0.06307 |
| 0.01 | 0.458193877 | 0.363 | 0.6910467 |
| 0.1 | 8.1672713 | 6.68 | 10.15468 |

Table 1 and Figure 3 shows the pressure drop for all pore shapes at different inlet velocities. For all types of pore shapes, as the inlet velocity increased, the pressure drop was increased.

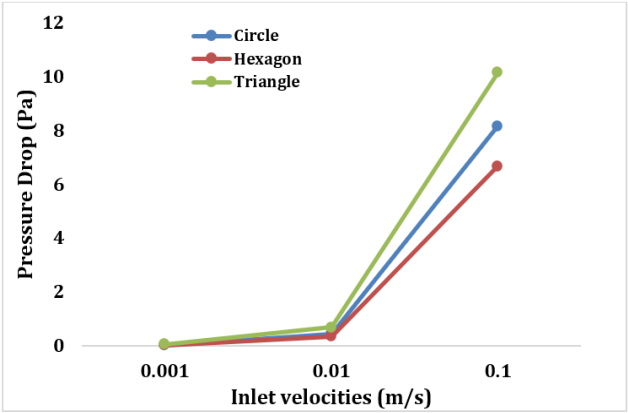


**Fig 3** Pressure drop at different velocities for each pore shape.

The pressure drop was created due to the higher velocity occurring at the inlet of the structure as the fluid flowing. Thus, the lower pressure was produced in the inlet region in contrast with the outlet region, which produced the higher pressure. Therefore, the difference eventually caused the pressure drop within the scaffold. Based on Figure 3, scaffold with triangle pore shape demonstrated the highest pressure drop at all inlet velocities.

The pressure drops obtained from CFD model analysisa were used to calculate the permeability value based on Darcy's Law equation. The permeability value for all scaffold were shown as in Table 2 and Figure 4. Based on the calculation, all scaffold demonstrated the permeability values that almost close to each other and the values were still within the range of principle permeability of bone, $0.22x10^{-8}m^2$ to $1.45x10^{-8}m^2$ (Vikingsson et al., 2015) or $0.5x10^{-8}m^2$ to $5x10^{-8}m^2$ (Singh et al., 2018). By increasing the inlet velocity, the permeability was decreased.

**Table 2** Permeability for each pore shape at different velocities.

| | Permeability ($m^2$) | | |
|---|---|---|---|
| **Velocity (m/s)** | **Circle** | **Hexagon** | **Triangle** |
| 0.001 | $3.0421x10^{-07}$ | $3.96691x10^{-07}$ | $2.02765x10^{-07}$ |
| 0.01 | $2.7912x10^{-07}$ | $3.52x10^{-07}$ | $1.8507x10^{-07}$ |
| 0.1 | $1.5659x10^{-07}$ | $1.92x10^{-07}$ | $1.2594x10^{-07}$ |

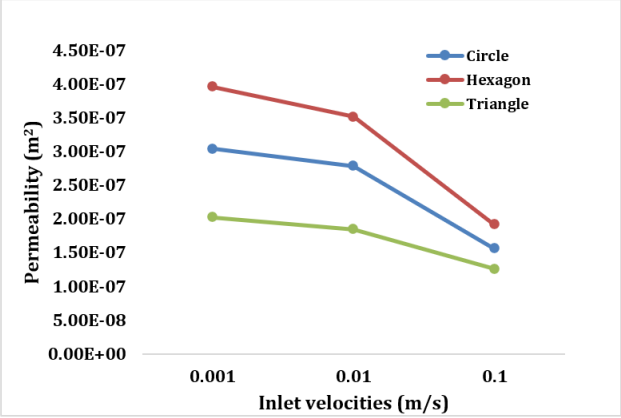


**Fig 4** Scaffold permeability at different inlet velocities.

Compared to all scaffolds, scaffold with hexagon pore shape showed the highest permeability value among the pore shapes. Scaffold with hexagon pore shapes demonstrated the lowest pressure drop due to the symmetries of the shape which allowed fluid to go through with less resistance. Meanwhile, scaffold with triangle pore shape demonstrated the lowest permeability value due to the sharp edges which gave more resistances to the fluid flow from inlet to the outlet. Besides, the bone growth rate increased when the width and curvature of pore was higher (Abbasi et al., 2020). Therefore, relevant permeability value would display a better result for the tissue growth in bone regeneration.

## CONCLUSION

We have successfully determined the permeability of scaffold with different pore shapes at a fixed diameter size of 2mm. By using Solidworks and Ansys, we able to conduct CFD Simulation to determine the pressure and velocity distribution within the three-unit cells scaffold. Based on the permeability value, hexagon pore shape exhibited the highest permeability followed by circle and triangle shape. Therefore, pore shape design will influence the permeability prediction that is crucial in determine the successful of a bone scaffold.

## ACKNOWLEDGEMENT

This work was supported by Universiti Teknologi Malaysia and Fundamental Research Grant Scheme (FRGS) grant **(**FRGS/1/2020/STG05/UTM/02/10**)** from Ministry of Education, Malaysia.

## REFERENCES

Abbasi, N., Hamlet, S., M. Love, R., Nguyen, N. 2020. Porous scaffolds for bone regeneration. Journal of Science: Advanced Materials and Devices, 5(1),1-9.

Daish, C., Blanchard, R., Gulati, K., Losic, D., Findlay. D., Harvie, D.J., Pivonka, P. 2017. Estimation of anisotropic permeability in trabecular bone based on microCT imaging and pore-scale fluid dynamics simulations. Bone Reports 1(6), 129-139.

Dias, M. R., Fernandes, P. R., Guedes, J. M., Hollister, S. J. 2012. Permeability analysis of scaffolds for bone tissue engineering. Journal of Biomechanics 45(6), 938-944.

Furumoto, T., Koizumi, A., Alkahari, M. R., Anayama, R., Hosokawa, A., Tanaka, R., Ueda, T, 2015. Permeability and strength of a porous metal structure fabricated by additive manufacturing. Journal of Materials Processing Technology 219,10-16.

Gómez, S., Vlad, M. D., López, J., Fernández, E. 2016. Design and properties of 3D scaffolds for bone tissue engineering. Acta Biomaterialia 42, 341-350.

Hutmacher, D. W., Schantz, J. T., Lam, C. X. F., Tan, K. C., Lim, T. C. 2007. State of the art and future directions of scaffold-based bone engineering from a biomaterials perspective. Journal of Tissue Engineering and Regenerative Medicine 1, 245-60.

Lesman, A., Blinder, Y., Levenberg, S. 2010. Modeling of flow-induced shear stress applied on 3D cellular scaffolds: Implications for vascular tissue engineering. Biotechnology and Bioengineering 105(3), 645-654.

Li, X., Liu, W., Sun, L., Aifantis, K. E., Yu, B., Fan, Y., Feng, Q., Cui, F., Watari, F. 2014. Resin composites reinforced by nanoscaled fibers or tubes for dental regeneration. Biomed. Res. Int. 2014, 542958.

Melchels, F. P., Tonnarelli, B., Olivares, A. L., Martin, I., Lacroix, D., Feijen, J., Grijpma, D.W. 2011. The influence of the scaffold design on the distribution of adhering cells after perfusion cell seeding. Biomaterials 32(11), 2878-2884.

O'brien, F. J. 2011. Biomaterials & scaffolds for tissue engineering. Materials Today, 14(3), 88-95.

Ochoa, I., Herrera, J., Aznar, J., Doblare, M., Yunos, D., Boccaccini, A. 2009. Permeability evaluation of45S5 Bioglasss-based scaffolds for bone tissue engineering. Journal of Biomechanics 42,257–260.

Pei, B., Wang, W., Fan, Y., Wang, X., Watari, F., Li, X. 2017. Fiber-reinforced scaffolds in soft tissue engineering. Regenerative Biomaterials 4(4), 257-268.

Podichetty, J., Madihally, S. 2014. Modelling of porous scaffold deformation induced by medium perfusion. Journal of Biomedical Materials Research B: Applied Biomaterials 102B, 737- 748.

Singh S. P., Shukla M., Srivastava R. K., Lattice modeling and CFD simulation for prediction of permeability in porous scaffolds. 2018. Materials Today: Proceedings, 5(9),18879-18886.

Truscello, S., Kerckhofs G., Van Bael, S., Pyka, G., Schrooten, J., Van Oosterwyck, H. 2012. Prediction of permeability of regular scaffolds for skeletal tissue engineering: a combined computational and experimental study. Acta biomaterialia 8(4),1648-58.

Vikingsson, L., Claessens, B., Gómez-Tejedor, J.A., Gallego Ferrer, G., Gómez Ribelles, J. L. 2015. Relationship between micro-porosity, water permeability and mechanical behavior in scaffolds for cartilage engineering. Journal of the Mechanical Behavior of Biomedical Materials 48,60-69.

Zhao, F., Vaughan, T. J., McNamara, L. M. 2016. Quantification of fluid shear stress in bonetissue engineering scaffolds with spherical and cubical pore architectures. Biomechanics and Modeling in Mechanobiology 15(3), 561-577.